



Microporous Metal-Organic Frameworks built from Rigid Tetrahedral Tetrakis(4-tetrazolylphenyl)silane Connectors

Journal:	<i>CrystEngComm</i>
Manuscript ID:	CE-COM-03-2014-000486.R1
Article Type:	Communication
Date Submitted by the Author:	03-Apr-2014
Complete List of Authors:	Timokhin, Ivan; Imperial College London, Department of Chemistry; University of Camerino, Dipartimento Scienze Chimiche White, Andrew; Imperial College London, Department of Chemistry Lickiss, Paul; Imperial College, Pettinari, Claudio; University of Camerino, Dipartimento Scienze Chimiche Davies, Robert; Imperial College London, Dept of Chemistry

COMMUNICATION

Microporous Metal-Organic Frameworks built from Rigid Tetrahedral Tetrakis(4-tetrazolyphenyl)silane Connectors

Cite this: DOI: 10.1039/x0xx00000x

Received 00th January 2012,
Accepted 00th January 2012I. Timokhin,^{a,b} A. J. P. White,^a P. D. Lickiss,^a C. Pettinari^b and R. P. Davies^{a*}

DOI: 10.1039/x0xx00000x

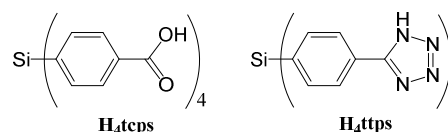
www.rsc.org/

Rigid tetrahedral ligands are of particular interest in Metal-Organic Framework (MOF) construction due to their highly branched nature, high symmetry and also their rarity. Within this context the silicon-centred linker tetrakis(4-tetrazolyphenyl)silane is shown to give porous networks exhibiting fluorite or garnet topology with copper(II), manganese(II) and cadmium(II) metal based nodes.

The field of metal-organic frameworks has grown exponentially over the past decade, with materials reported with extremely high porosities and potential applications in areas as diverse as gas storage, gas separation, catalysis and drug delivery to name but a few.^{1,2} The design of the organic connector plays a key role in the design of new MOF materials and the modification of existing ones.³ However, despite recent advances the preparation of rigid tetrahedral organic-connectors for MOF building remains somewhat problematic due to the challenging syntheses of these ligands.³ We have sought to address this by pioneering the use of silicon as a tetrahedral centre, which can be readily substituted to form tetrahedral and other rigid and highly branched linkers.⁴⁻⁷ In addition to their facile synthetic accessibility these ligands have, in some cases, been shown to exhibit subtly different chemical and physical properties to their carbon-based analogs leading to novel structural motifs.⁸

Research on silicon connectors for MOF construction to date has primarily focussed upon the preparation and use of polytopic-carboxylates such as tetrakis(carboxyphenyl)silane (tcps).^{4-6,9-12} In addition, work in our group has recently led to the first report of a polytopic tetrazolyl silicon based ligand, tetrakis(4-tetrazolyphenyl)silane (ttps). H₄ttps was demonstrated to react with copper(II) chloride to give a highly porous network (**IMP-16**, hereafter known as **IMP-16Cu**) which exhibits *flu* topology.⁸ Unique to **IMP-16Cu** is the orientation of the square-planar {Cu₄(μ⁴-Cl)}⁺ nodes which lie perpendicular to each other and therefore differ from the nodal co-planarity exhibited in the carbon-centred analog Cu₄(ttpm)₂·0.7CuCl₂ (ttpm = tetrakis(4-

tetrazolyphenyl)methane) reported by Long and co-workers.¹³ This can be explained by the increased rotational freedom about the Si-Ar bonds in ttps compared to conformationally restricted C-Ar bond rotation in the ttpm analog. The work now presented further explores the use of the ttps ligand in MOF construction with four new MOFs reported based on this connector.



Solvothermal reaction between H₄ttps and MnCl₂·4H₂O in the presence of HCl, DMF and methanol at 80 °C gave pale yellow cubic crystals of [H(Mn₄Cl)(ttps)₂(DMF)₄]₂₀DMF (**IMP-16Mn**). Single-crystal X-ray diffraction studies reveal a porous three dimensional network built from chloride-centred square-planar {Mn₄(μ⁴-Cl)}⁺ nodes, each of which is bridged by eight tetrazolate groups from eight separate ttps ligands (Fig. 1a). The sixth coordination site on each copper is occupied by a DMF molecule. The structure is therefore isomorphous with **IMP-16Cu** and represents, as far as we are aware, only the second example of such a {Mn₄(μ⁴-Cl)}⁺ node in MOF chemistry,¹⁴ and the first in combination with a T_d ligand. Mn-Cl bonds lie in the range 2.6998(14) to 2.7459(17) Å and Mn-N bonds in the range 2.199(4) to 2.214(4) Å. These distances are longer than the comparable Cu-N and Cu-Cl bonds in **IMP-16Cu**⁸ resulting in an elongation of the cell length parameter and an increase in overall cell volume (see Table 1). The combination of cubic eight-coordinate metal-based nodes with tetrahedral ttps ligands gives rise to a 4,8 connected net with the fluorite (*flu*) topology (Fig. 1b and 1d).

Table 1 Comparison of the unit-cell parameters and gas sorption data of **IMP-16Cu/Mn**

	IMP-16Cu^{a,8}	IMP-16Mn^a
<i>a</i> , Å	18.5153(3)	18.8266(5)
<i>c</i> , Å	25.0576(7)	25.4638(17)
<i>V</i> , Å ³	8590.2(4)	9025.4(8)
SAV ^b , Å ³	6384 (74.3%)	6693 (74.2%)
Internal Surface area:		
Langmuir, m ² g ⁻¹	3123	2956
BET, m ² g ⁻¹	2665	2510

^a Tetragonal crystal system ($a = b$; $\alpha = \beta = \gamma = 90^\circ$). ^b solvent-accessible volume (SAV) calculated using the "SOLV" algorithm implemented in the PLATON package¹⁵.

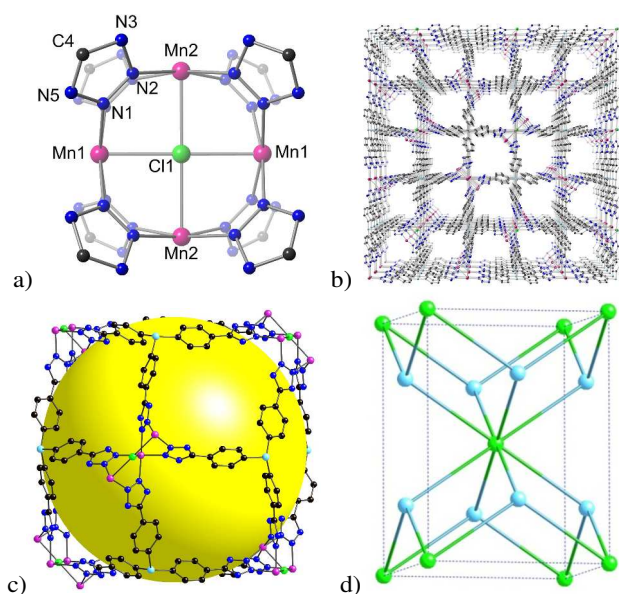


Fig. 1 a) Ball and stick representations of the coordination environment around the $Mn_4Cl(tetrazolate)_8$ node (colour scheme: Mn, purple; Cl, green; N, blue; C, black). b) View of a section of **IMP-16Mn** from the 001 direction (hydrogen atoms and solvent molecules have been removed for clarity). c) Diagrammatic picture of one of the cavities in **IMP-16Mn**. d) Schematic representation of one unit-cell of the network showing the *flu* topology (Si nodes, light blue; Cu_4Cl nodes, green).

The structure of **IMP-16Mn** is highly porous with a solvent-accessible volume (SAV), as calculated from the crystal structure using the PLATON routine¹⁵, of 6693 Å³ per unit cell or 74.2% (assuming removal of all DMF solvent from the structure). This is slightly lower than that reported for **IMP-16Cu**, but is significantly more than that reported for the $Cu_4(tpm)_2 \cdot 0.7CuCl_2$ (66.9%)¹³. The internal cavity size in **IMP-16Mn** is 2.1 nm and the framework window sizes are 8.5 x 8.5 Å² and 9.5 x 9.5 Å² (atom-to-atom distances, Figure 1c). The pores are initially filled with disordered DMF solvent molecules (40 per unit cell – see ESI), but these can be removed to enable gas uptake studies. Experimental gas sorption data obtained on an evacuated sample shows a reversible Type I adsorption isotherm (Figure 2) and a saturation amount of 710 cm³ g⁻¹ at 0.9 bar. This is congruent

with the PLATON calculations, being slightly lower than that reported for **IMP-16Cu** (740 cm³ g⁻¹ at 0.9 bar). The apparent surface area as determined by the BET and Langmuir methods is 2510 and 2956 m² g⁻¹ respectively (Table 1).

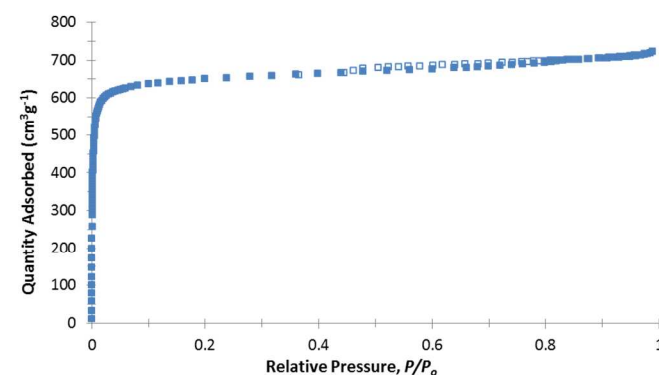


Fig. 2 Nitrogen gas sorption isotherm for **IMP-16Mn** measured at 77K. Filled and empty symbols represent adsorption and desorption data respectively

The bulk purity of **IMP-16Mn** and the repeatability of its synthesis were further verified with powder diffraction studies (see ESI). Attempts to prepare the analogous **IMP-16Cd** MOF using $CdCl_2$ as the metal containing reagent were unsuccessful, instead yielding a mix of microcrystalline products of undeterminable structure. Nevertheless gas sorption studies on these 'cadmium MOF' product(s) revealed microporosity with a N₂ saturation amount of 420 cm³ g⁻¹ at 0.9 bar and BET and Langmuir calculated internal surface areas of 1725 and 1248 m² g⁻¹ respectively (see ESI).

A series of metal nitrate salts were also treated with the H_4ttps connector in order to probe the role of the halide anion (or absence thereof) in the construction of metal tetrazolyl MOFs. Thus reaction of H_4ttps with the metal(II) nitrate salts, $Mn(NO_3)_2 \cdot 4H_2O$, $Cu(NO_3)_2 \cdot 2H_2O$ or $Cd(NO_3)_2 \cdot 4H_2O$, in a mixture of DMF and methanol at 80 °C gave the respective crystalline products **IMP-17Mn**, **IMP-17Cu** and **IMP-17Cd**. Single crystal X-ray diffraction studies reveal isostructural MOF materials of formula $M_6(tps)_3(DMF)_6$ ($M = Mn, Cu, Cd$). These **IMP-17** MOFs differ from **IMP-16** being built from trimetallic nodes, comprising of a linear arrangement of metal centres bridged by the tetrazolyl groups of six different *ttps* ligands to yield an octahedral metal-based nodal unit (Figure 3a). The central metal dication within the building unit (Mn1, Figure 2a) is octahedrally coordinated by the nitrogen atoms of six different *ttps* connectors, whilst the terminals metal centres (Mn2) are facially coordinated both by three nitrogen atoms from three *ttps* ligands and three oxygen atoms of three solvent molecules (DMF or methanol). Metal – metal distances and mean metal-nitrogen bonding distances for the different MOFs are summarised in Table 2. Similar linear trimetallic units are relatively well known in metal azolate frameworks.¹⁶ The combination of the tetrahedral organic linkers and inorganic octahedral vertices gives rise to a 4,6-connected three-dimensional microporous structure (Figure 3b) based on the

garnet (*gar*) net (Figure 3d) with the topology directly comparable to the $\text{Al}_2\text{Si}_3\text{O}_{12}$ part of a garnet. The *gar* net is uncommon in MOF chemistry: previously reported examples include $\text{Mn}_6(\text{tppm})_3$ ¹³ and $\text{In}_2\text{Zn}_3(\text{imidazolate})_{12}$ (ZIF-5).¹⁷ The largest enclosed space within the **IMP-17** structures is approximately 14 Å in diameter (atom-to-atom distance, see Figure 3c).

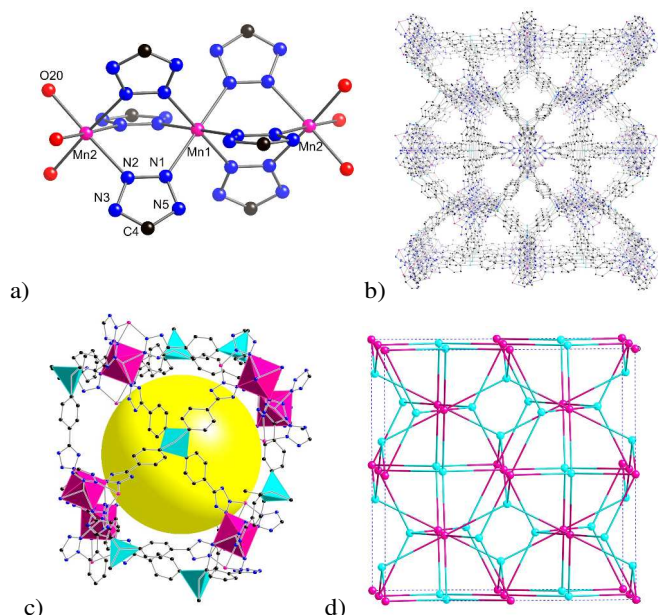


Fig. 3 a) Ball and stick representations of the coordination environment around the $\text{Mn}_3(\text{tetrazolate})_6$ node (colour scheme: Mn, purple; O, red; N, blue; C, black). b) View of a section of **IMP-17Mn** from the 010 direction (hydrogen atoms and solvent molecules have been removed for clarity). c) Diagrammatic picture of one of the cavities in **IMP-17Mn**. d) Schematic representation of one unit-cell of the network showing the *gar* topology (Si nodes, light blue; Mn_3 nodes, purple).

Comparison of the crystallographic parameters for all three **IMP-17** MOFs shows an increase in cell length and volume with increasing ionic radius of the metal ($\text{Cu(II)} < \text{Mn(II)} < \text{Cd(II)}$). The single-crystal X-ray structures indicate a high degree of porosity for these structures, with PLATON calculated¹⁵ solvent-accessible volumes (SAV) exceeding 70% (assuming removal of all co-ordinated and non-coordinated solvent from the structures, see Table 2). However, in contrast to **IMP-16** these MOFs all show limited structural stability: **IMP-17Cd** and **IMP-17Cu** undergo decomposition within 24 hours when stored on the open bench, and all **IMP-17** MOFs decomposed rapidly under evacuation to form amorphous non-porous solids. Gas sorption measurements on **IMP-17Mn** showed a N_2 saturation amount of just $20 \text{ cm}^3 \text{ g}^{-1}$ at 0.9 bar indicating an almost complete loss of porosity on evacuation.

Table 2 Comparison of the unit-cell parameters and selected distances in **IMP-17Mn/Cd/Cu**

	IMP-17Mn	IMP-17Cd	IMP-17Cu
$a, \text{Å}$	36.7051(15)	36.97447(15)	36.1906(18)
$V, \text{Å}^3$	49452(6)	50548.2(4)	47401(7)
M...M distance, Å	4.055	4.110	3.734
Mean M-N distance, Å	2.227	2.335	2.091
SAV ^b , Å ³	35350(71.5%)	36998.7(73.2%)	34270 (72.3%)

^a Cubic crystal system ($a = b = c$; $\alpha = \beta = \gamma = 90^\circ$). ^b solvent-accessible volume (SAV) calculated using the "SOLV" algorithm implemented in the PLATON package¹⁵.

In summary, the coordination chemistry of the novel silicon-based tetrahedral tps ligand has been further explored and MOFs based on this ligand reported displaying *flu* or *gar* topological nets. The chloride centred tetrametallic nodes in **IMP-16** lead to robust materials that can withstand evacuation and demonstrate high levels of porosity and gas sorption capacity. The trimetallic nodes which form the octahedral vertices within the **IMP-17** series of MOFs also give rise to microporous structures, however these frameworks readily decompose under evacuation making them unsuitable for gas storage or sorting applications.

The authors acknowledge UNICAM (I.T.) for the support of this research. In addition we thank the EPSRC UK National Crystallography Service at the University of Southampton (and P. N. Horton in particular) for the collection of the crystallographic data for **IMP-17Cu**.

Notes and references

^a Department of Chemistry, Imperial College London, South Kensington, London, SW7 2AZ, UK; E-mail: r.davies@imperial.ac.uk

^b Scuola del Farmaco e dei Prodotti della Salute, Università degli Studi di Camerino, via S. Agostino 1, I-62032 Camerino, MC, Italy.

† Electronic Supplementary Information (ESI) available: Full experimental details of the syntheses, characterisation data and the crystallographic protocols employed in this study and powder X-ray diffraction and thermogravimetric analysis plots. For ESI and crystallographic data in CIF or other electronic format see DOI: -----/-----/

‡ The SQUEEZE routine of PLATON¹⁵ was employed to treat the regions of diffuse solvent in all structures. *Crystal data for IMP-16Mn*: $\text{C}_{68}\text{H}_{61}\text{ClMn}_4\text{N}_{36}\text{O}_4\text{Si}_2 \cdot 20(\text{C}_3\text{H}_7\text{NO})$, $M = 3219.84$, tetragonal, $P4_2/mmm$ (no. 136), $a = b = 18.8266(5)$, $c = 25.4638(17)$ Å, $V = 9025.4(8)$ Å³, $Z = 2$ (D_{2h} symmetry), $D_c = 1.185 \text{ g cm}^{-3}$, $\mu(\text{Cu-K}\alpha) = 3.085 \text{ mm}^{-1}$, $T = 173 \text{ K}$, pale yellow cubes, Oxford Diffraction Xcalibur PX Ultra diffractometer; 4666 independent measured reflections ($R_{\text{int}} = 0.0845$), F^2 refinement, $R_1(\text{obs}) = 0.0841$, $wR_2(\text{all}) = 0.2943$, 2075 independent observed absorption-corrected reflections [$|F_o| > 4\sigma(|F_o|)$, $2\theta_{\text{max}} = 145^\circ$], 121 parameters. CCDC 989922.

IMP-17Mn: $\text{C}_{40}\text{H}_{44}\text{Mn}_2\text{N}_{20}\text{O}_4\text{Si} \cdot 28(\text{C}_3\text{H}_7\text{NO})$, $M = 3053.60$, cubic, $Ia-3d$ (no. 230), $a = 36.7051(15)$ Å, $V = 49452(6)$ Å³, $Z = 24$ (-3 symmetry), $D_c = 2.461 \text{ g cm}^{-3}$, $\mu(\text{Cu-K}\alpha) = 3.956 \text{ mm}^{-1}$, $T = 173 \text{ K}$, colourless blocks, Oxford Diffraction Xcalibur PX Ultra diffractometer; 4003 independent

measured reflections ($R_{\text{int}} = 0.2211$), F^2 refinement, $R_1(\text{obs}) = 0.1447$, $wR_2(\text{all}) = 0.4057$, 786 independent observed absorption-corrected reflections [$|F_o| > 4\sigma(|F_o|)$, $2\theta_{\text{max}} = 144^\circ$], 116 parameters. CCDC 989923.

IMP-17Cd: $\text{C}_{40}\text{H}_{44}\text{Cd}_2\text{N}_{20}\text{O}_4\text{Si}$, $M = 2291.38$, cubic, $Ia-3d$ (no. 230), $a = 36.97447(15) \text{ \AA}$, $V = 50548.2(4) \text{ \AA}^3$, $Z = 24$ (-3 symmetry), $D_c = 1.807 \text{ g cm}^{-3}$, $\mu(\text{Cu-K}\alpha) = 5.047 \text{ mm}^{-1}$, $T = 173 \text{ K}$, colourless blocks, Oxford Diffraction Xcalibur PX Ultra diffractometer; 4182 independent measured reflections ($R_{\text{int}} = 0.0793$), F^2 refinement, $R_1(\text{obs}) = 0.0528$, $wR_2(\text{all}) = 0.1348$, 3535 independent observed absorption-corrected reflections [$|F_o| > 4\sigma(|F_o|)$, $2\theta_{\text{max}} = 145^\circ$], 172 parameters. CCDC 989924.

IMP-17Cu: $\text{C}_{28}\text{H}_{16}\text{Cu}_2\text{N}_{16}\text{O}_4\text{Si}$, $M = 795.74$, cubic, $Ia-3d$ (no. 230), $a = 36.1906(18) \text{ \AA}$, $V = 47401(7) \text{ \AA}^3$, $Z = 24$ (-3 symmetry), $D_c = 0.669 \text{ g cm}^{-3}$, $\mu(\text{Cu-K}\alpha) = 0.580 \text{ mm}^{-1}$, $T = 100 \text{ K}$, blue-green prisms, Rigaku AFC12 (Right) diffractometer; 3498 independent measured reflections ($R_{\text{int}} = 0.116$), F^2 refinement, $R_1(\text{obs}) = 0.136$, $wR_2(\text{all}) = 0.440$, 1134 independent observed absorption-corrected reflections [$|F_o| > 4\sigma(|F_o|)$, $2\theta_{\text{max}} = 50^\circ$], 104 parameters. CCDC 989925.

1. H. Furukawa, K. E. Cordova, M. O'Keeffe and O. M. Yaghi, *Science*, 2013, **341**, 974-+.
2. 2012 Metal-Organic Frameworks Issue. *Chem. Rev.* 2012, **112**, 673-1268; [Http://pubs.acs.org/toc/chreay/112/2](http://pubs.acs.org/toc/chreay/112/2)
3. S. L. Qiu and G. S. Zhu, *Coord. Chem. Rev.*, 2009, **253**, 2891-2911.
4. R. P. Davies, R. J. Less, P. D. Lickiss, K. Robertson and A. J. P. White, *Inorg. Chem.*, 2008, **47**, 9958-9964.
5. R. P. Davies, R. Less, P. D. Lickiss, K. Robertson and A. J. P. White, *Crystal Growth & Design*, 2010, **10**, 4571-4581.
6. R. P. Davies, P. D. Lickiss, K. Robertson and A. J. P. White, *Aust. J. Chem.*, 2011, **64**, 1237-1244.
7. R. P. Davies, P. D. Lickiss, K. Robertson and A. J. P. White, *Crystengcomm*, 2012, **14**, 758-760.
8. I. Timokhin, J. B. Torres, A. J. P. White, P. D. Lickiss, C. Pettinari and R. P. Davies, *Dalton Trans.*, 2013, **42**, 13806-13808.
9. J. B. Lambert, Z. Q. Liu and C. Q. Liu, *Organometallics*, 2008, **27**, 1464-1469.
10. M. Zhang, Y.-P. Chen and H.-C. Zhou, *Crystengcomm*, 2013, **15**, 9544-9552.
11. Y.-S. Xue, L. Zhou, M.-P. Liu, S.-M. Liu, Y. Xu, H.-B. Du and X.-Z. You, *CrystEngComm*, 2013, **15**, 6229-6236.
12. J. M. Gotthardt, K. F. White, B. F. Abrahams, C. Ritchie and C. Boskovic, *Crystal Growth & Design*, 2012, **12**, 4425-4430.
13. M. Dinca, A. Dailly and J. R. Long, *Chem. Eur. J.*, 2008, **14**, 10280-10285.
14. M. Dinca, A. Dailly, Y. Liu, C. M. Brown, D. A. Neumann and J. R. Long, *J. Am. Chem. Soc.*, 2006, **128**, 16876-16883.
15. A. L. Spek, *PLATON99, A Multipurpose Crystallographic Tool*, (1999) Utrecht University, Utrecht, The Netherlands.
16. J.-P. Zhang, Y.-B. Zhang, J.-B. Lin and X.-M. Chen, *Chem. Rev.*, 2011, **112**, 1001-1033.
17. K. S. Park, Z. Ni, A. P. Côté, J. Y. Choi, R. Huang, F. J. Uribe-Romo, H. K. Chae, M. O'Keeffe and O. M. Yaghi, *PNAS*, 2006, **103**, 10186-10191.
- 18.

Microporous Metal-Organic Frameworks built from Rigid Tetrahedral Tetrakis(4-tetrazolylphenyl)silane Connector

A series of related MOFs built from the rigid tetrahedral H_4ttps ligand with Mn(II), Cu(II) or Cd(II) metal based nodes exhibiting rare fluorite or garnet topologies have been synthesised and characterised and are compared to one another.

